

# New Insights into Global Spin Alignment of Vector Mesons Using Relativistic Heavy-Ion Collisions from STAR

Baoshan Xi<sup>1,\*</sup> for the STAR Collaboration

<sup>1</sup>Fudan University, 220 Handan Rd., Yangpu District, Shanghai(200433), CHINA

**Abstract.** In these proceedings, we present new measurements from STAR of the global spin alignment( $\rho_{00}$ ) of  $\phi$  mesons in Au+Au collisions at  $\sqrt{s_{NN}} = 19.6, 14.6$  GeV using BES-II data and of  $J/\psi$  mesons in isobar collisions  $^{96}_{44}\text{Ru} + ^{96}_{44}\text{Ru}$  and  $^{96}_{40}\text{Zr} + ^{96}_{40}\text{Zr}$  at  $\sqrt{s_{NN}} = 200$  GeV. The energy-dependent spin alignment for  $\phi$  mesons from BES-II data is consistent with that published from BES-I and showcases a significant improvement in precision. We performed a new measurement assessing the rapidity dependence of  $\phi$  meson  $\rho_{00}$ , and our findings are consistent with theoretical predictions. The global spin alignment of  $J/\psi$  mesons with respect to first order event plane aligns with a value of  $1/3$  within the statistical error. Additionally, we discuss the procedure of measuring the global spin alignment of  $\rho^0$  mesons at RHIC and provide the projection for errors.

## 1 Introduction

In non-central heavy-ion collisions, a substantial amount of angular momentum is generated when two nuclei pass each other at near-light speed. This angular momentum results in the formation of a vorticity field within the system. Through spin-orbital coupling within this vorticity field, quarks can become polarized along the direction of the angular momentum[1, 2]. This quark-level polarization along a global direction is eventually reflected in the polarization of hyperons or the spin alignment of vector mesons, both of which can be measured in experiments.

The global spin alignment of particles produced in heavy-ion collisions can provide valuable insights into the strong force field and the properties of the quark-gluon plasma. Recently, the STAR collaboration measured the global spin alignment of  $\phi$  and  $K^{*0}$  in Au+Au collisions using data from the first phase of the RHIC Beam Energy Scan program (BES-I) [3]. In these measurements, the global spin alignment ( $\rho_{00}$ ) of  $K^{*0}$  was found to be consistent with  $1/3$ , whereas the  $\rho_{00}$  of  $\phi$  significantly exceeded  $1/3$ . The large signal for  $\phi$  meson cannot be explained by conventional mechanisms but might be attributed to the influence of vector meson force fields. The observed signal of this global spin alignment aligns with a model incorporating  $\phi$  meson field coupling to the  $s$  and  $\bar{s}$  quarks[4], offering new insights into strong interactions.

Our interpretation gains depth from the inclusion of BES-II data collected at collision energies of  $\sqrt{s_{NN}} = 14.6$  and  $19.6$  GeV. With significantly larger statistics and the incorporation

---

\*e-mail: xibaoshan@fudan.edu.cn

37 of a new event plane detector (EPD), these measurements substantially enhance detection ac-  
 38 curacy. Exploring the relationship between global spin alignment and rapidity could provide  
 39 intriguing insights into the nuances of the fluctuating local strong force field, as emphasized  
 40 in the theoretical prediction[6].

41 A notable aspect allowing the assessment of contributions from the fluctuating strong  
 42 force field in theory is the composition of  $\phi$  mesons, which are made up of  $s\bar{s}$  quarks from the  
 43 same flavor family. This uniqueness makes the global spin alignment measurement for  $J/\psi$   
 44 particularly interesting, given that  $J/\psi$  is composed of  $c\bar{c}$  quarks, which also belong to the  
 45 same flavor family. In contrast, the  $\rho^0$  meson, unlike  $\phi$  and  $J/\psi$ , comprises a mixture of quark  
 46 flavors  $(u\bar{u} - d\bar{d})/\sqrt{2}$ . Due to its short lifetime,  $\rho^0$  mesons are continuously destroyed and  
 47 regenerated. These factors make it less optimal as a probe for local fluctuations in the strong  
 48 force field. However, the global spin alignment of  $\rho^0$  mesons holds significant implications  
 49 for Chiral Magnetic Effect (CME) analyses[7, 8].

50 These studies, incorporating more differential measurements and exploring vector mesons  
 51 with various quark contents, are geared towards comprehending the influence of vector meson  
 52 force fields on the evolution of matter produced in heavy-ion collisions. By introducing new  
 53 particle species and its decay channels, researchers can gain insights into the complex effects  
 54 of in-medium interactions and hadronization mechanisms on global spin alignment.

## 55 2 Analysis method

56 We reconstructed vector mesons and obtained the distribution of  $\cos\theta^*$ , where  $\theta^*$  is angle  
 57 between the polarization direction  $\hat{L}$  and the momentum direction of a daughter particle in  
 58 the rest frame of the parent vector meson. We use Eq. (1) to fit the  $\cos\theta^*$  distribution, where  
 59 the upper sign is used for  $\phi$  and  $\rho^0$  meson, and the lower sign is used for  $J/\psi$ [9].

$$\frac{dN}{d\cos\theta^*} = N_0 \times \left[ (1 \mp \rho_{00}^{obs}) \pm (3\rho_{00}^{obs} - 1) \cos^2\theta^* \right] \quad (1)$$

60 where  $N_0$  is the normalization factor, and  $\rho_{00}^{obs}$  is the observed global spin alignment. From  
 61 an experimental standpoint,  $\rho_{00}$  is reflected in the directional tendency of emitted decaying  
 62 daughters. When  $\rho_{00} = 1/3$ ,  $\cos\theta^*$  is uniformly distributed, indicating no global spin align-  
 63 ment. Conversely, a deviation of  $\rho_{00}$  from  $1/3$  results in a non-uniform distribution of  $\cos\theta^*$ .

64 To ensure the accurate determination of the physical global spin alignment, it is crucial  
 65 to apply additional corrections for detector effects. We calculate detector efficiency using  
 66 embedding technique[10]. Finite acceptance in pseudorapidity could introduce artificial sig-  
 67 nals, and a finite event plane resolution might smear the signal strength. Both aspects have  
 68 been corrected as outlined in[11]. To validate the effectiveness of our correction method, we  
 69 conducted simulation experiments considering limited detector acceptance and event plane  
 70 resolution. The final corrected  $\rho_{00}$  value exhibited excellent agreement with the initial input  
 71  $\rho_{00}$  value.

## 72 3 Results

73 The dependence of  $\phi$ 's global spin alignment on the transverse momentum  $p_T$ , was investi-  
 74 gated in Au+Au collisions at  $\sqrt{s_{NN}} = 14.6$  GeV during BES-II, as illustrated in the left panel  
 75 of Figure 1. In the figure, black symbols denote results from measurements relative to the  
 76 first order event plane, while red symbols indicate results relative to the second order event  
 77 plane. The first order EP gives better correlation to direction of  $\hat{L}$ , while second order EP

78 gives better precision results. Notably, there is no significant difference observed in the measured  $\rho_{00}$  values within uncertainties. The BES-II results substantially reduced measurement  
 79 errors and are consistent with those from BES-I[3].  
 80

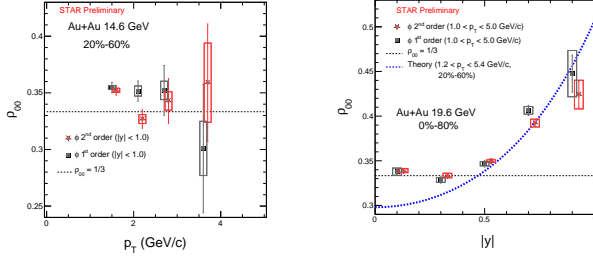


Figure 1: Left panel : global spin alignment of  $\phi$  as a function of  $p_T$  for Au+Au collisions at  $\sqrt{s_{NN}} = 14.6$  GeV, obtained with BES-II data. Right panel : rapidity dependence of global spin alignment for Au+Au collisions at  $\sqrt{s_{NN}} = 19.6$  GeV. For both panels, the black and red symbols represent results relative to first order and second order EPs respectively.

81 A new study examining the rapidity dependence of global spin alignment was conducted  
 82 using BES-II data. The right panel of Figure 1 displays the results from Au+Au collisions  
 83 at 19.6 GeV. In the figure, black symbols results relative to first order EP and red symbols  
 84 relative to second order EP. All results exhibit significant rapidity dependence. The theoretical  
 85 prediction for rapidity dependence at 19.6 GeV displays similar trend in data for  $|y| > 0.5$ ,  
 86 depicted by the blue curve in the right figure[5, 6]. This observed phenomenon may be  
 87 attributed to larger fluctuations of the strong force field in the meson's rest frame enhanced  
 88 by its motion in directions perpendicular to that of global angular momentum[6].

89 In Figure 2, we present the global spin alignment measurements of  $J/\psi$  using the first-  
 90 order event plane in isobar collisions at  $\sqrt{s_{NN}} = 200$  GeV. The red symbols represent the  
 91 results for Ru+Ru collisions, while the blue symbols represent the results for Zr+Zr collisions.  
 92 Across central to peripheral collisions, the data are consistent with  $1/3$  within the  
 93 margin of error. Notably, the ALICE collaboration observed that signals of global spin alignment  
 94 of  $J/\psi$  are smaller than  $1/3$  in PbPb collisions[12], while the global spin alignment of  
 95  $D^*$  at high  $p_T$  is greater than  $1/3$ [13]. These findings provide additional insights for theorists  
 96 to unravel the underlying mechanisms governing global spin alignment induced by the strong  
 97 force field.

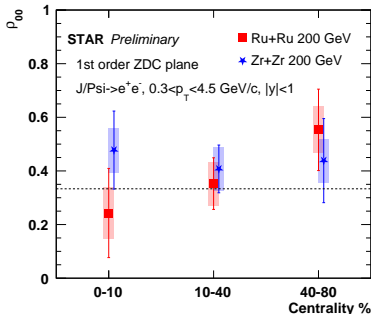
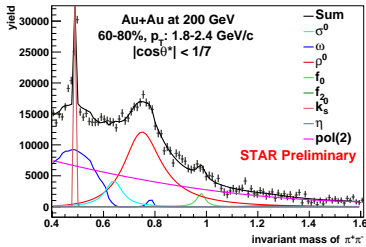


Figure 2: Global spin alignment of  $J/\psi$ . The red and blue symbols represent the result of Ru+Ru and Zr+Zr, respectively.

In a recent phenomenological study, the relation between the global spin alignment of  $\rho^0$  mesons and CME observable  $\Delta\gamma_{112}$  was explored[7, 8]. Conversely, the influence of  $\rho^0$  meson  $\rho_{00}$  on the CME-background-control method, such as the spectator/participant plane ratio of the CME observables or the event shape engineering, requires further dedicated investigation. The study[7, 8] revealed a clear dependence of CME observables on  $\rho^0$  meson's  $\rho_{00}$ . Investigating the global spin alignment of  $\rho^0$  mesons is crucial to understanding impact on CME observables. However, extracting  $\rho^0$  meson's  $\rho_{00}$  is complicated by the cocktail background in the invariant mass dis-

112 tribution. We reconstructed the invariant mass spectrum through the decay channel  $\rho^0 \rightarrow$   
 113  $\pi^+\pi^-$  with Au+Au and isobar collisions at  $\sqrt{s_{NN}} = 200$  GeV. The spectrum involves contri-  
 114 butions from 7 particles:  $\omega, \rho^0, f_0, f_2, \sigma^0, k_s^0$  and  $\eta$ . This complexity makes the extraction of  
 115  $\rho^0$  yield highly challenging. In Figure 3, We present the cocktail fitting results of a  $\cos\theta^*$   
 116 bin for  $\rho^0$  with  $p_T$  of 1.8-2.4 GeV/c in Au+Au collisions. This study is currently in progress.  
 117 Currently, our estimation suggests that the absolute uncertainty of  $\rho_{00}$  that can be obtained  
 118 from combined Au+Au collision data in 2023 and 2025 is on the order of 0.01.



**Figure 3.** Cocktail fitting of yield in a  $\cos\theta^*$  bin for  $\rho^0$  meson, where the red curve represents the signal of  $\rho^0$ . The plot is for  $p_T$  within 1.8-2.4 GeV/c and centrality within 60-80% in Au+Au collisions at  $\sqrt{s_{NN}} = 200$  GeV.

## 119 4 Summary

120 In these proceedings, we investigated the global spin alignment of vector mesons, including  
 121  $\phi$  and  $J/\psi$ . From measurements in Au+Au collisions at  $\sqrt{s_{NN}} = 19.6$  GeV, we uncovered  
 122 intriguing, strong dependency on rapidity for  $\phi$  global spin alignment, shedding light on the  
 123 intricate interplay between the fluctuating strong force field and meson spin alignment. The  
 124  $J/\psi$  global spin alignment with respect to first order event plane is found to be consistent with  
 125  $1/3$  within error. We further looked into the feasibility of extracting  $\rho_{00}$  for  $\rho^0$  meson, which  
 126 can have potential impact on our understanding of the Chiral Magnetic Effect in nuclear  
 127 collisions.

## 128 References

- 129 [1] Z. T. Liang and X. N. Wang, Phys. Rev. Lett. **94**, 102301 (2005) [erratum: Phys. Rev.  
 130 Lett. **96**, 039901 (2006)].  
 131 [2] Z. T. Liang and X. N. Wang, Phys. Lett. B **629**, 20 (2005).  
 132 [3] M. S. Abdallah *et al.* (STAR Collaboration), Nature **614**, 7947, 244 (2023).  
 133 [4] X. L. Sheng, L. Oliva and Q. Wang, Phys. Rev. D **101**, 096005 (2020), [erratum: Phys.  
 134 Rev. D **105**, 099903 (2022)].  
 135 [5] X. L. Sheng, L. Oliva, Z. T. Liang, Q. Wang and X. N. Wang, Phys. Rev. Lett. **131**,  
 136 042304 (2023).  
 137 [6] X. L. Sheng, S. Pu and Q. Wang, Phys. Rev. C **108**, 054902 (2023).  
 138 [7] D. Shen, J. Chen, A. Tang and G. Wang, Phys. Lett. B **839**, 137777 (2023).  
 139 [8] A. H. Tang, Chin. Phys. C **44**, 054101 (2020).  
 140 [9] P. Faccioli, C. Lourenco, J. Seixas and H. K. Wohri, Eur. Phys. J. C **69**, 657 (2010).  
 141 [10] B. I. Abelev *et al.* (STAR Collaboration), Phys. Rev. C **81**, 024911 (2010).  
 142 [11] A. H. Tang, B. Tu, C. S. Zhou, Phys. Rev. C **98**, 044907 (2018), [erratum: Phys. Rev. C  
 143 **107**, 039901 (2023)].  
 144 [12] S. Acharya *et al.* (ALICE Collaboration), Phys. Rev. Lett. **131**, 042303 (2023).  
 145 [13] L. Micheletti, Investigating the early magnetic field of QGP via heavy-flavour polar-  
 146 isation studies with ALICE , Quark Matter, 2023, [https://indico.cern.ch/event/1139644/  
 147 contributions/5540118/](https://indico.cern.ch/event/1139644/contributions/5540118/).